

# The relationship between grain shape and interstellar polarization

N. V. Voshchinnikov\* and I. S. Yakovlev

*Astronomy Department and Sobolev Astronomical Institute, St. Petersburg University, Universitetskii prosp., 28, St. Petersburg, 198504 Russia.*

We analyze the effects of grain shape and orientation on the parameters of the interstellar linear-polarization curve. The consideration is performed for partially aligned prolate and oblate spheroidal particles with aspect ratios  $a/b$  varying from 1.1 to 10.

## LINEAR POLARIZATION: OBSERVATIONS

The phenomenon of interstellar linear polarization is caused by the linear dichroism of the interstellar medium due to the presence of non-spherical oriented grains. Non-spherical particles produce differing extinction of light depending on the orientation of the electric vector of incident radiation relative to the particle axis. The spectral dependence of polarization in the visible part of the spectrum  $P(\lambda)$  is described by the Serkowski empirical formula (see, e.g., [1])

$$P(\lambda)/P_{\max} = \exp[-K \ln^2(\lambda_{\max}/\lambda)], \quad (1)$$

where  $K$  is the coefficient,  $P_{\max}$  the maximum degree of polarization, and  $\lambda_{\max}$  the wavelength corresponding to it. From the analysis of observational data for several hundred stars, it has been found that the upper limit on the ratio of  $P_{\max}$  to the colour excess  $E(B - V)$  is [1]

$$P_{\max}/E(B - V) \lesssim 9\%/mag. \quad (2)$$

This ratio determines the polarizing efficiency of the interstellar medium towards a particular star.

A relation has been established between the total-to-selective extinction ratio  $R_V$  and  $\lambda_{\max}$  ( $R_V = (5.6 \pm 0.3) \lambda_{\max}$ ,  $\lambda_{\max}$  in  $\mu\text{m}$ ) and regional variations of  $R_V$  and  $\lambda_{\max}$  (see Fig. 4.13 in [2]). The increase of  $R_V$  and  $\lambda_{\max}$  is usually attributed to the growth of grain size, although both parameters also depend on the degree and direction of grain alignment [3].

In [3], an anticorrelation has been noted between the observed polarizing efficiency and  $\lambda_{\max}$ , i.e., a larger value of  $\lambda_{\max}$  corresponds to a smaller value of  $P_{\max}/E(B - V)$ . Using the model of infinite cylinders, this fact has been interpreted as the decrease of the angle between the line of sight and the magnetic field direction  $\Omega$ .

To test this hypothesis, we have used recent data of Efimov [4], who fitted the multi-wavelength polarimetric observations for 105 stars. We have chosen 76 stars located in the galactic plane ( $|b| \lesssim 20^\circ$ ) with distances  $D \lesssim 1$  kpc. The observed values of  $P_{\max}/E(B - V)$

\*Corresponding author: Nikolai Voshchinnikov (nvv@astro.spbu.ru)

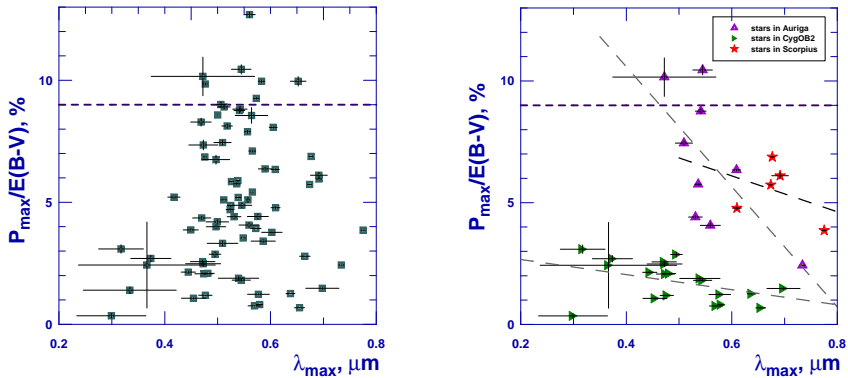


**Figure 1.** Polarizing efficiency of the interstellar medium as a function of wavelength, where interstellar linear polarization is maximized. Data are shown for 76 stars located within 1000 pc (left) and, separately, for stars in Auriga, Cygnus, and Scorpius (right). The horizontal line is the observational upper limit as given by Eq. 2. Dashed lines are linear fits. Data were taken from [4].

versus  $\lambda_{\max}$  (we have used the Whittet fit from [4]) are plotted in Fig. 1 (left panel). It can be seen that there is no correlation. However, for stars more or less closely located on the sky, a systematic trend toward smaller polarizing efficiency for larger  $\lambda_{\max}$  is obvious (right panel of Fig. 1).

To interpret the observations, one needs to utilize a model of rotating partially aligned non-spherical grains. Such a model was recently developed and applied in the simultaneous interpretation of the observed interstellar extinction and polarization curves for certain stars [5, 6]. The shape of the grains in the spheroidal model is characterized by one parameter: the ratio of the major and minor semi-axes  $a/b$ . Note that previous modelling of interstellar polarization with spheroids has included non-rotating particles with  $a/b \lesssim 2$  (see [7, 8, 9]).

## SPHEROIDAL MODEL OF INTERSTELLAR DUST

We use the model of homogeneous spheroids with a power-law size distribution ( $n(r_V) \propto r_V^{-q}$ ) with imperfect Davis-Greenstein (IDG) orientation (see [5, 6] for details). Spheroids are characterized by their type (prolate or oblate), the aspect ratio  $a/b$ , and size parameter  $r_V$  (radius of a sphere whose volume is equal to that of a non-spherical particle). For a given wavelength  $\lambda$ , the extinction and polarization cross sections  $\langle C_{\text{ext}} \rangle_\lambda$  and  $\langle C_{\text{pol}} \rangle_\lambda$  are obtained by averaging of the cross sections over the size distribution and grain orientations. The direction of grain orientation is described by the angle  $\Omega$  (angle between the line of sight and the magnetic field direction,  $0^\circ \leq \Omega \leq 90^\circ$ ). The value  $\Omega = 90^\circ$  corresponds to the case when the particle rotation plane contains the light propagation vector  $\mathbf{k}$ , which gives the maximum degree of linear polarization. For  $\Omega = 0^\circ$ , the light falls perpendicular to the particle rotation plane and from symmetry reasons the net degree of polarization produced is zero.

The IDG mechanism is described by the function  $f(\xi, \beta)$  depending on the alignment parameter  $\xi$  and the precession angle  $\beta$

$$f(\xi, \beta) = \frac{\xi \sin \beta}{(\xi^2 \cos^2 \beta + \sin^2 \beta)^{3/2}}. \quad (3)$$

The parameter  $\xi$  depends on the particle size  $r_V$ , the imaginary part of the grain magnetic susceptibility  $\chi''$ , gas density  $n_H$ , the strength of magnetic field  $B$ , and temperatures of dust  $T_d$  and gas  $T_g$ ,

$$\xi^2 = \frac{r_V + \delta_0(T_d/T_g)}{r_V + \delta_0}, \quad \delta_0 = 8.23 \times 10^{23} \frac{\varkappa B^2}{n_H T_g^{1/2} T_d} [\mu\text{m}]. \quad (4)$$

Our model has the following main parameters: the minimum and maximum grain radii  $r_{V,\min}$  and  $r_{V,\max}$ , the power index  $q$ , and the degree ( $\delta_0$ ) and direction ( $\Omega$ ) of grain alignment.

## RESULTS AND DISCUSSION

We made calculations for polydisperse ensembles of spheroids consisting of astronomical silicate (astrosil [10]) and amorphous carbon (AC-Be [11]). The size-distribution parameters were chosen so as to give the ratio  $R_V \approx 3.1 - 3.2$  for particles with  $a/b \approx 1$ . This occurs if  $r_{V,\min} = 0.010 \mu\text{m}$ ,  $r_{V,\max} = 0.25 \mu\text{m}$ , and  $q = 2.5$  for particles from astrosil and  $r_{V,\min} = 0.001 \mu\text{m}$ ,  $r_{V,\max} = 0.25 \mu\text{m}$ , and  $q = 4.0$  for particles from AC-Be. Some results are plotted in Figs. 2 and 3. They show the polarizing efficiency  $P_{\max}/E(B-V)$  as a function of the angle  $\Omega$  and the degree of alignment  $\delta_0$ . The colour excess  $E(B-V)$  was found by averaging over the B and V filter passbands taken from [12].

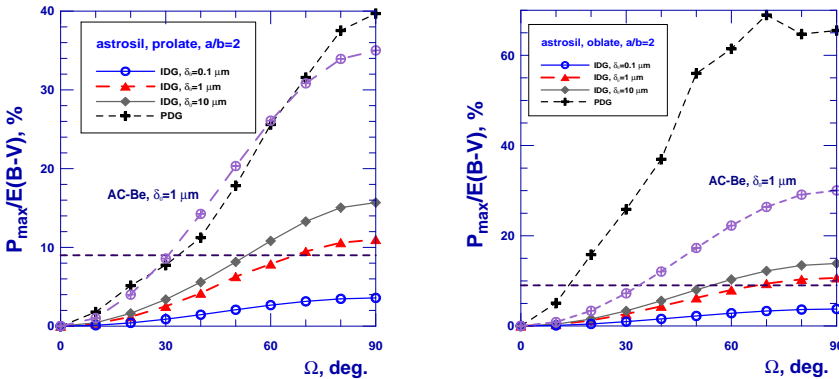


**Figure 2.** Polarizing efficiency dependence on angle between the line of sight and the magnetic field. The results are plotted for prolate (left) and oblate (right) spheroids from astrosil with imperfect (IDG) and perfect (PDG) Davis-Greenstein orientation. The horizontal line shows the observational upper limit as given by Eq. 2.

As expected, the polarizing efficiency grows with increasing  $\Omega$ ,  $\delta_0$ , and  $a/b$  (Figs. 2 and 3). At the same time, a difference is seen between the polarizing properties of the prolate and oblate spheroids. Partially aligned oblate particles only slightly polarize transmitted radiation if  $\Omega \lesssim 40^\circ - 50^\circ$  (Fig. 2, right panel). This is true for silicate and carbon particles. If the aspect ratios of prolate and oblate particles are the same, then similar polarization can be reached if the degree of alignment for oblate particles is higher than that for prolate particles.

Note that  $\lambda_{\max}$  is mainly determined by grain size and shape and weakly depend on the alignment parameters. The resulting relationships will be applied in detailed comparison of

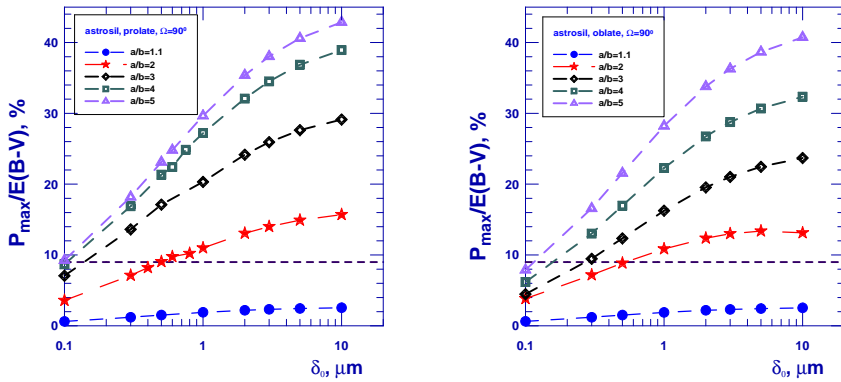


**Figure 3.** Polarizing efficiency dependence on the degree of alignment. The results are plotted for prolate (left) and oblate (right) spheroids from astrosil with IDG orientation. The horizontal line shows the observational upper limit as given by Eq. 2.

the theory with observations.

**Acknowledgments:** The work was partly supported by the grants RFBR 07-02-00831, RFBR 10-02-00593a, NTP 2.1.1/665 and NSh 1318.2008.2.

## REFERENCES

- [1] K. Serkowski, D.S. Mathewson and V.L. Ford. Wavelength dependence of interstellar polarization and ratio of total to selective ratio. *ApJ* **196** (1975).
- [2] D.C.B. Whittet. *Dust in the Galactic Environments*. Institute of Physics Publishing, Bristol (2nd ed.) (2003).
- [3] N.V. Voshchinnikov. Determination of dust properties and magnetic fields from polarimetric and photometric observations of stars. *Astron. Nachr.* **310** (1989).
- [4] Yu.S. Efimov. Interstellar polarization: new approximation. *Bull. CrAO* **105** (2009).
- [5] N.V. Voshchinnikov and H.K. Das. Modelling interstellar extinction and polarization with spheroidal grains. *JQSRT* **109** (2008).
- [6] H.K. Das, N.V. Voshchinnikov, and V.B. Il'in. Interstellar extinction and polarization — A spheroidal dust grain approach perspective. *MNRAS* **404** (2010).
- [7] P.G. Martin. *Cosmic Dust*. Oxford Univ. Press, Oxford (1978).
- [8] C. Rogers and P.G. Martin. On the shape of interstellar grains. *ApJ* **228** (1979).
- [9] B.T. Draine and A.A. Fraisse. Polarized far-infrared and submillimeter emission from interstellar dust. *ApJ* **696** (2009).
- [10] B.T. Draine. Scattering by interstellar dust grains. II. X-rays. *ApJ* **598** (2003).
- [11] V.G. Zubko, V. Menella, L. Colangeli, and E. Bussoletti. Optical constants of cosmic carbon analogue grains - I. Simulation of clustering by a modified continuous distribution of ellipsoids. *MNRAS* **282** (1996).
- [12] V. Strazys. *Multicolor Stellar Photometry*. Pachart Publ. House, Tucson (1992).